Genes & Diseases (2021) 8, 918–930

Available online at www.sciencedirect.com

ScienceDirect

journal homepage: http://ees.elsevier.com/gendis/default.asp

FULL LENGTH ARTICLE

Argonaute (AGO) proteins play an essential role in mediating BMP9-induced osteogenic signaling in mesenchymal stem cells (MSCs)

Yukun Mao [a,b], Na Ni [b,c], Linjuan Huang [b,d], Jiaming Fan [b,c], Hao Wang [b,c], Fang He [b,c], Qing Liu [b,e], Deyao Shi [b,f], Kai Fu [a,b], Mikhail Pakvasa [b,g], William Wagstaff [b], Andrew Blake Tucker [b,g], Connie Chen [b], Russell R. Reid [b,g], Rex C. Haydon [b], Sherwin H. Ho [b], Michael J. Lee [b], Tong-Chuan He [b,g], Jian Yang [h], Le Shen [b,g], Lin Cai [a,**], Hue H. Luu [b,*]

[a] *Departments of Spine Surgery and Musculoskeletal Tumor, and Neurosurgery, Zhongnan Hospital of Wuhan University, Wuhan, Hubei Province, 430072, PR China*
[b] *Molecular Oncology Laboratory, Department of Orthopaedic Surgery and Rehabilitation Medicine, The University of Chicago Medical Center, Chicago, IL 60637, USA*
[c] *Ministry of Education Key Laboratory of Diagnostic Medicine, and the School of Laboratory Medicine, Chongqing Medical University, Chongqing, 400016, PR China*
[d] *Departments of Nephrology, and Obstetrics and Gynecology, The First Affiliated Hospital of Chongqing Medical University, Chongqing, 400016, PR China*
[e] *Department of Spine Surgery, Second Xiangya Hospital, Central South University, Changsha, Hunan Province, 410011, PR China*
[f] *Department of Orthopaedic Surgery, Union Hospital of Tongji Medical College, Huazhong University of Science and Technology, Wuhan, Hubei Province, 430022, PR China*
[g] *Section of Plastic Surgery and Laboratory of Craniofacial Biology and Development, and Section of Surgical Research, Department of Surgery, The University of Chicago Medical Center, Chicago, IL 60637, USA*
[h] *Department of Biomedical Engineering, Materials Research Institute, The Huck Institutes of the Life Sciences, The Pennsylvania State University, University Park, PA 16802, USA*

Received 9 March 2021; received in revised form 4 April 2021; accepted 16 April 2021
Available online 13 May 2021

* Corresponding author. Molecular Oncology Laboratory, Department of Orthopaedic Surgery and Rehabilitation Medicine, The University of Chicago Medical Center, 5841 South Maryland Avenue, MC3079, Chicago, IL 60637, USA. Fax: +(773) 834 4598.
** Corresponding author. Department of Spine Surgery and Musculoskeletal Tumor, Zhongnan Hospital, Wuhan University, Wuhan, Hubei Province, 430071, China.
E-mail addresses: orthopedics@whu.edu.cn (L. Cai), hluu@bsd.uchicago.edu (H.H. Luu).
Peer review under responsibility of Chongqing Medical University.

https://doi.org/10.1016/j.gendis.2021.04.004

KEYWORDS
Argonaute (AGO) proteins;
BMP9;
Bone formation;
Lineage-specific differentiation;
Mesenchymal stem cells;
miRNA biogenesis;
Osteogenic signaling

Abstract As multipotent progenitor cells, mesenchymal stem cells (MSCs) can renew themselves and give rise to multiple lineages including osteoblastic, chondrogenic and adipogenic lineages. It's previously shown that BMP9 is the most potent BMP and induces osteogenic and adipogenic differentiation of MSCs. However, the molecular mechanism through which BMP9 regulates MSC differentiation remains poorly understood. Emerging evidence indicates that noncoding RNAs, especially microRNAs, may play important roles in regulating MSC differentiation and bone formation. As highly conserved RNA binding proteins, Argonaute (AGO) proteins are essential components of the multi-protein RNA-induced silencing complexes (RISCs), which are critical for small RNA biogenesis. Here, we investigate possible roles of AGO proteins in BMP9-induced lineage-specific differentiation of MSCs. We first found that BMP9 upregulated the expression of *Ago1, Ago2* and *Ago3* in MSCs. By engineering multiplex siRNA vectors that express multiple siRNAs targeting individual *Ago* genes or all four *Ago* genes, we found that silencing individual *Ago* expression led to a decrease in BMP9-induced early osteogenic marker alkaline phosphatase (ALP) activity in MSCs. Furthermore, we demonstrated that simultaneously silencing all four *Ago* genes significantly diminished BMP9-induced osteogenic and adipogenic differentiation of MSCs and matrix mineralization, and ectopic bone formation. Collectively, our findings strongly indicate that AGO proteins and associated small RNA biogenesis pathway play an essential role in mediating BMP9-induced osteogenic differentiation of MSCs.

Introduction

As multipotent progenitor cells, mesenchymal stem cells (MSCs) can renew themselves and give rise to multiple lineages including chondrogenic, adipogenic, osteogenic, and myogenic lineages.[1–5] Osteoblastic lineage-specific differentiation of MSCs is regulated by numerous major signaling pathways.[2,6–13] Bone morphogenetic proteins (BMPs) are considered as the most potent osteoinductive factors.[14–16] BMPs are members of the transforming growth factor β (TGF-β) superfamily,[2,14,15] and at least 14 BMPs have been identified in humans and rodents.[14,15,17] We conducted a comprehensive analysis of the 14 types of human BMPs, and identified the least known BMP9 as one of the most potent osteogenic BMPs in MSCs.[14,16,18–21] We further demonstrated that, unlike other osteogenic BMPs, BMP9 is refractory to the inhibitory effect exerted by the potent naturally occurring antagonist noggin,[22] and that the TGF-β/BMP type I receptors ALK1 and ALK2 are essential for BMP9 osteogenic signaling[23] and regulating downstream target genes in MSCs.[24–31] Nonetheless, the molecular mechanisms underlying BMP9-induced osteogenic differentiation of MSCs are not fully understood.

For the past 20 years, significant progress has been in genome-wide transcriptomic studies, indicating that noncoding RNAs (ncRNAs) may play critical roles in most if not all aspects of cellular processes under physiological and/or pathologic conditions,[32–34] since only less than 2% of the human genome encodes proteins, while eukaryotic genomes are pervasively transcribed.[34,35] Noncoding RNAs are divided into small ncRNAs (<200 nt) and long ncRNAs or lncRNAs (>200 nt).[33] In fact, small ncRNAs, e.g., microRNAs (miRNAs) and small interfering RNAs (siRNAs), have gained a lot of attention since their discoveries.[36,37] It has been reported that ncRNAs, especially microRNAs, may play important roles in regulating MSC differentiation and bone formation.[38,39]

MicroRNAs (miRNAs) are small ncRNAs of ~22 nucleotides and attenuate gene expression by guiding Argonaute (AGO) proteins to target mRNAs that are completely or partially complementary with miRNAs.[40–42] The biogenesis of miRNAs starts with longer primary transcripts (i.e., pri-miRNAs) with a 60-120 nt RNA hairpin structure.[41] The pri-miRNAs are then cleaved by Drosha and Dicer, yielding ~70 nt precursor miRNAs (i.e., pre-miRNAs) and eventually 22 nt mature miRNAs.[41] Mature miRNAs usually down-regulate gene expression post-transcriptionally through binding of target mRNAs in association with the AGO-containing RNA-induced silencing complex (RISC).[41] Small interfering RNAs (siRNAs) are also processed and subsequently silence target transcripts through interacting with the AGO2-containing RISC system.[43–45] Thus, the AGO proteins are essential players in processing and biogenesis of small RNAs (smRNAs) in mammalian cells. AGOs use single-stranded small nucleic acids as guides and bind to complementary sequences in RNA targeted for modulation.[41] There are at least four AGO proteins, namely, AGO1 to AGO4, in humans and mice.[41,46]

In this study, we investigate potential roles of AGO proteins in BMP9-induced lineage-specific differentiation of MSCs. Using our recently developed FASMi technology,[47] we engineered the multiplex siRNA vectors to express multiple siRNAs targeting individual *Ago* genes or all four *Ago* genes in either recombinant adenoviral or retroviral vector

system. We demonstrated that BMP9 up-regulated the expression of *Ago*1, *Ago*2 and *Ago*3 in MSCs; and that silencing individual *Ago* expression led to a decrease in BMP9-induced alkaline phosphatase (ALP) activity in MSCs. We further demonstrated that simultaneous silencing of all four *Ago* genes effectively diminished BMP9-induced adipogenic and osteogenic differentiation of MSCs and matrix mineralization *in vitro,* and ectopic bone formation *in vivo*. Collectively, our findings indicate that AGO proteins and associated microRNA biogenesis pathway play an important role in mediating BMP9-induced osteogenesis in MSCs.

Material and methods

Cell culture and chemicals

HEK-293 cells were obtained from ATCC (Manassas, VA). HEK-293 derivative lines 293pTP and RAPA cells were previously described.[48,49] Reversibly immortalized mouse bone marrow stromal cells (imBMSCs) were previously characterized.[50] All cell lines were maintained in DMEM containing 10% fetal bovine serum (FBS; Gemini Bio-Products, West Sacramento, CA), supplemented with 100U/mL penicillin and 100 μg/mL streptomycin, and incubated at 37 °C in 5% CO_2 as described.[13,51–54] Unless indicated otherwise, all other chemicals were purchased from Sigma–Aldrich (St. Louis, MO, USA) or Thermo Fisher Scientific (Waltham, MA, USA).

Construction and generation of recombinant adenoviruses AdBMP9, AdGFP, AdRFP, AdR-sim*Ago*1, AdR-sim*Ago*2, AdR-sim*Ago*3 and AdR-sim*Ago*4

Recombinant adenoviruses were constructed by using the AdEasy technology as described.[55,56] Briefly, for making the overexpression adenoviruses, the coding regions of human BMP9, eGFP and RFP were PCR amplified, subcloned into the adenoviral shuttle vector, and used to generate recombinant adenoviruses in HEK293, 293pTP, or RAPA cells as described,[13,28,57–59] subsequently designated as AdBMP9, AdGFP and AdRFP.

The multiplex siRNA expressing adenoviruses were constructed by using our recently developed FAMSi system.[47] Briefly, three siRNAs were designed to target the coding region of each *Ago* member by using Invitrogen's BLOCK-IT RNAi Designer program. The siRNA sites were assembled into the FAMSi vector system, and subsequently cloned into a homemade adenoviral vector for generating adenoviruses as described.[47,58,60–62] The resultant adenoviruses were designated as AdR-sim*Ago*1, AdR-sim*Ago*2, AdR-sim*Ago*3, and AdR-sim*Ago*4. All PCR amplified fragments were verified by DNA sequencing. The cloning construction details are available upon request.

It is noteworthy that AdBMP9 and AdR-sim*Ago* viruses also express eGFP and RFP as infection tracking markers, respectively. For all adenoviral infections, AdGFP and AdRFP were used as control viruses for mock infection as described.[22,29,30,63–69] For all adenoviral infections, polybrene (final concentration at 5 μg/mL) was added to enhance infection efficiency as described.[70]

Construction of the retroviral vector pSEB-sim*Ago*2134 and the establishment of stable imBMSC cells expressing sim*Ago*2134 line imBMSC-sim*Ago*2134

To silence all four *Ago* members, a multiplex siRNA construct, pSiEB-sim*Ago*2134, was assembled by using the FAMSi system.[47] The retroviral vector pSiEB-sim*Ago*2134 expresses two siRNAs targeting *Ago*2 and one siRNA each targeting *Ago*1, *Ago*3, and *Ago*4. The previously engineered pSEB-siControl vector was used a negative control as described.[47,58,61] The retroviral vector pSiEB-sim*Ago*2134 or pSiEB-siControl was co-transfected with retroviral packaging plasmids into HEK-293 cells to produce retrovirus supernatants, which were used to infect subconfluent imBMSC cells to establish imBMSC-sim*Ago*2134 or imBMSC-siControl stable line upon blasticidin S selection (final concentration at 5 μg/mL), as previously described.[69,71–75]

RNA extraction and touchdown quantitative PCR (TqPCR)

Total RNA isolated with the TRIZOL Reagent (Invitrogen, Carlsbad, CA) was subjected to reverse transcription reactions using hexamer and M-MuLV Reverse Transcriptase (New England Biolabs, Ipswich, MA,USA). The RT cDNA products were used as qPCR templates. The qPCR primers were designed by using the Primer3 Plus,[76] and are listed in Table S1. The quantitative PCR analysis was performed using our previously optimized TqPCR protocol.[17,62,63,77] Briefly, SYBR Green qPCR reactions (Bimake, Houston, TX) were set up according to manufacturer's instructions. The cycling program was set up as follows: 95 °C × 3 min for 1 cycle; 95 °C × 20 s, 66 °C × 10 s per cycle, then −3 °C per cycle for 4 cycles; followed by 95 °C × 10 s, 55 °C × 15 s, and 70 °C × 1 s for 40 cycles. *Gapdh* was used as a reference gene. Relative expression for all samples was calculated by using the $2^{-\Delta\Delta Ct}$ method as described.[58,72,77]

Alkaline phosphatase (ALP) activity assays

Exponentially growing imBMSC cells and/or their derivative lines were plated in 24-well plates and co-infected with the indicated adenoviral vectors. At days 3, 5, or 7, the infected cells were subjected to either quantitative ALP activity assessment using the modified Great Escape SEAP chemiluminescence assay kit (BD Clontech) and/or qualitative histochemical staining of ALP activity as previously described.[47,52,57,78,79] Each assay condition was conducted in triplicate.

In vitro matrix mineralization assay

Exponentially growing imBMSCs cells were plated in 24-well plates, co-infected with the indicated adenoviruses, and cultured with 10% FBS DMEM containing ascorbic acid (50 mg/mL) and β-glycerophosphate (10 mM). At days 14

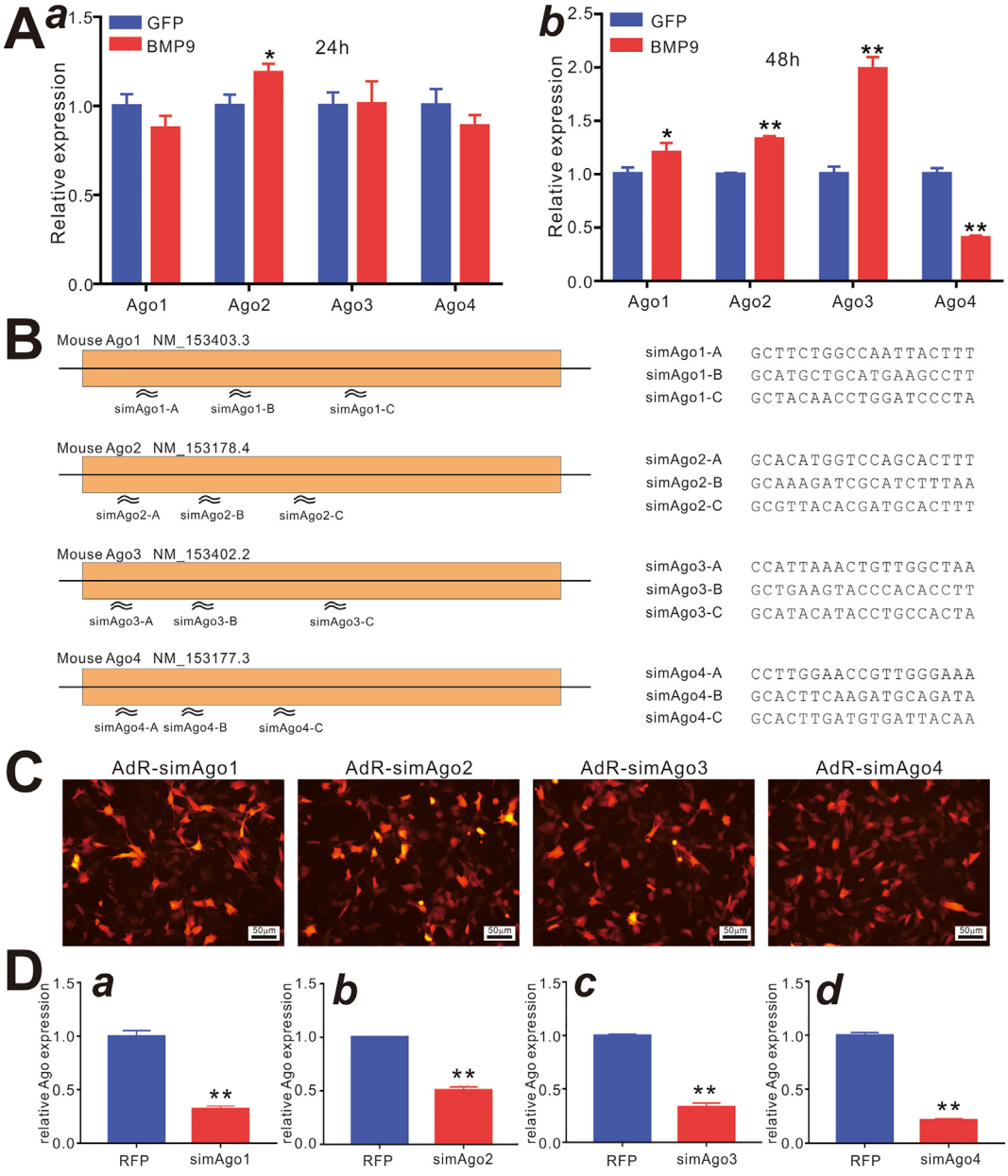

Figure 1 BMP9 impacts on the expression of *Ago* genes, which can be effectively silenced through adenoviral vector-mediated expression of *Ago*-specific siRNAs in MSCs. **(A)** Subconfluent imBMSCs were infected with Ad-BMP9 (BMP9) and AdGFP control (GFP). At 24 h (***a***) and 48 h (***b***) after infection, total RNA was isolated and subjected to TqPCR analysis of *Ago1*, *Ago2*, *Ago3* and *Ago4* expression. *Gapdh* was used as a reference gene. *, $P < 0.05$, and **, $P < 0.01$ when compared with that of the AdGFP group. Each assay was done in triplicate. **(B)** Location and sequence features of the siRNAs that target the coding regions of mouse *Ago1*, *Ago2*, *Ago3*, *Ago4*. The siRNAs targeting individual *Ago* gene transcript were cloned into recombinant adenoviral vectors using our recently established FAMSi technique, resulting in the adenoviruses designated as AdR-simAgo1, AdR-simAgo2, AdR-simAgo3 and AdR-simAgo4, respectively. **(C)** AdR-simAgo viruses can transduce MSCs with high efficiency. Subconfluent imBMSCs were infected with AdR-sim*Ago*1, AdR-sim*Ago*2, AdR-sim*Ago*3, or AdR-sim*Ago*4. At 48 h after infection, RFP signal was recorded. Representative images are shown. **(D)** AdR-simAgo vectors effectively silence the expression of respective *Ago* genes in MSCs. Subconfluent imBMSCs were infected with the indicated AdR-sim*Ago* viruses, or AdRFP. At 48 h after infection, total RNA was isolated and subjected to TqPCR analysis of expression of mouse *Ago1* (**a**), *Ago2* (**b**), *Ago3* (**c**), and *Ago4* (**d**). *Gapdh* was used as a reference gene. Each assay was done in triplicate. **, $P < 0.01$ when compared with that of the AdGFP group.

and 21, mineralized matrix nodules were stained by Alizarin Red S staining as described.[59,80–82] Briefly, the cells were fixed with 2.5% glutaraldehyde for 10 min, washed with PBS (pH adjusted to 4.2) twice, and then incubated with 2% Alizarin Red S for 30 min at room temperature. The stained mineral deposits were recorded under bright field microscopy. Each assay condition was done in triplicate.

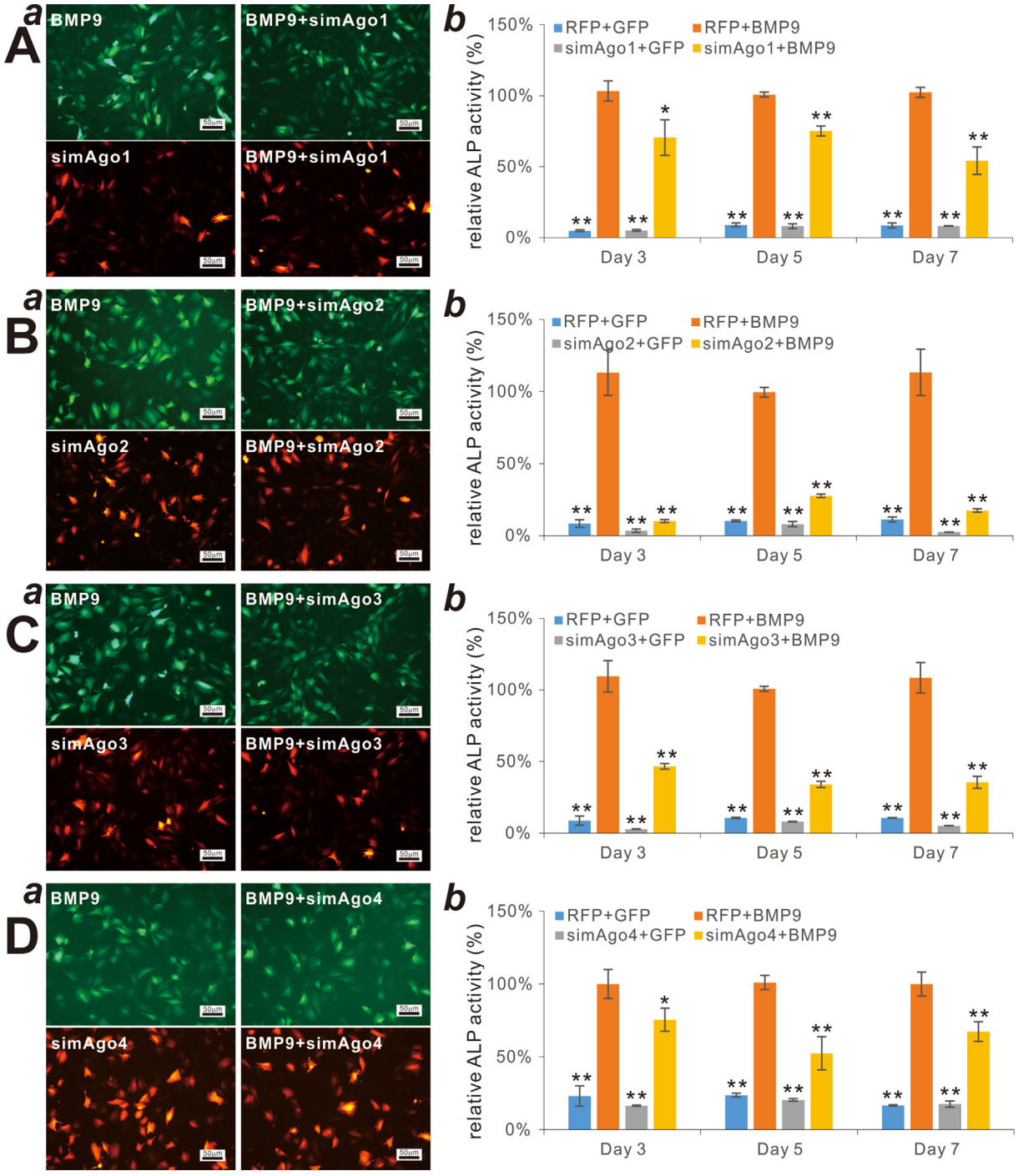

Figure 2 Silencing Ago expression leads to a decrease in BMP9-induced ALP activity in MSCs. Subconfluent imBMSCs were co-infected with Ad-RFP or Ad-BMP9 and AdGFP, AdR-simAgo1 **(A)**, AdR-simAgo2 **(B)**, AdR-simAgo3 (**C**), or AdR-simAgo4 **(D)**. At 48 h post infection, GFP and RFP signals were recorded, and representative images are shown in (***a***). At the indicated time points, ALP activity was quantitatively assessed (***b***). Each assay condition was performed in triplicate. *, $P < 0.05$ and **, $P < 0.01$, compared with that of the RFP + BMP9 group at respective time points.

Oil Red O staining assay

Exponentially growing imBMSCs cells were seeded in 24-well cell culture plates and co-infected with the indicated adenoviruses. At day 7, the cells were subjected to Oil Red O staining as described.[29,57,69,83–85] Briefly, the cells were fixed with 10% formalin at room temperature for 10min, washed with PBS, and stained with freshly prepared Oil Red-O solution at room temperature for 60 min, followed by washing with distilled water. The staining of lipid droplets was recorded under a bright field microscope. Each assay condition was performed in triplicate.

Subcutaneous stem cell implantation and ectopic bone formation

All animal use and care in this study followed the approved protocol by the Institutional Animal Care and Use Committee. All experimental procedures were carried out according to the approved guidelines. Subcutaneous stem cell implantation procedure was performed as previously described.[22,50,59,86–88] Briefly, subconfluent imBMSC-siControl and imBMSC-sim*Ago*2134 cells were infected with AdGFP or AdBMP9 for 36 h. The infected cells were collected, resuspended in PBS, and subcutaneously injected into the flanks of athymic nude mice (Envigo/Harlan Research Laboratories; $n = 5$/group, 6–8-week old; 2×10^6 cells in 50 μl per injection site). At three weeks after implantation, the mice were sacrificed, and masses at implantation sites were recovered for μCT and histologic analyses.

Micro-computed tomographic (μCT) analysis

The retrieved bony masses were fixed in 10% PBS-buffered formalin and subjected to μCT imaging by using the GE triumph (GE Healthcare) trimodality preclinical imaging system. All imaging data were analyzed with the Amira 6.0 (Visage Imaging, Inc.). The average bone volume was determined as previously described.[89–92]

Hematoxylin and eosin (H & E) and Masson's trichrome staining

The retrieved samples were decalcified and paraffin embedded. Serial sections of the embedded samples were subjected to H & E staining and Masson's trichrome staining as previously described.[19,93–96]

Statistical analysis

The quantitative assays were performed in triplicate and/or repeated in three independent batches. Statistical differences between samples were determined by *t*-test or ANOVA. The $P < 0.05$ was defined as statistically significant.

Results

BMP9 regulates the expression of *Ago* family members in MSCs

We first analyzed the effect of BMP9 on the expression of *Ago* family members in MSCs. At 24 h of AdBMP9 infection, only *Ago*2 was up-regulated upon BMP9 stimulation (Fig. 1A, panel a). However, at 48 h after BMP9 stimulation, *Ago*1, *Ago*2 and *Ago*3 were significantly up-regulated while *Ago*4 was down-regulated. While the detailed regulatory mechanism remains to be fully investigated, these results indicate that *Ago* family members play an important role in mediating BMP9 signaling in MSCs.

To further investigate the role of the *Ago* members in BMP9 signaling, we designed a series of siRNAs that target four *Ago* genes, each of which was targeted by three siRNAs (Fig. 1B). The three siRNAs (e.g., sim*Ago*) for each *Ago* gene were assembled into a recombinant adenoviral vector, and the generated adenoviruses were shown to transduce MSCs with high efficiency (Fig. 1C). Quantitative qPCR analysis

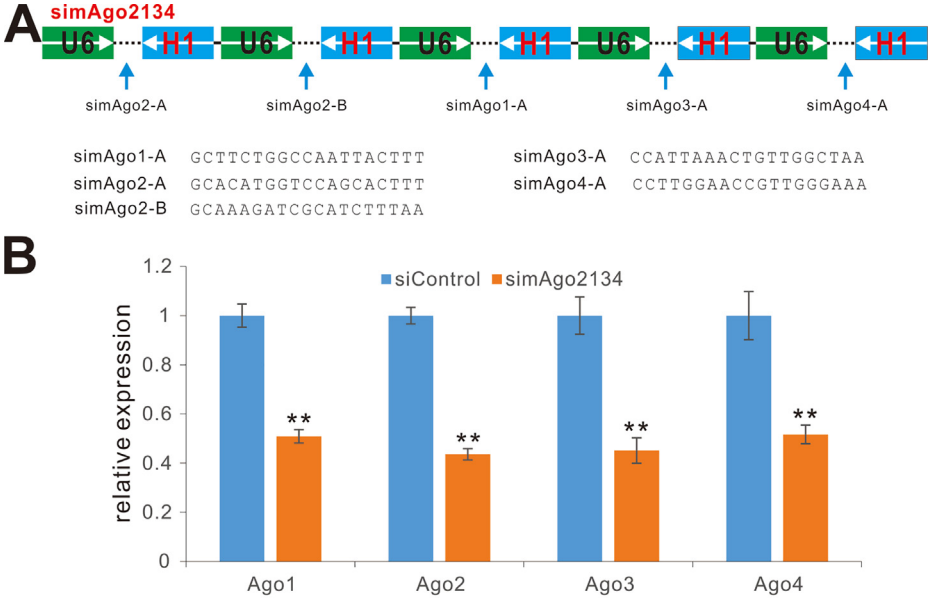

Figure 3 Characterization of a retroviral vector that simultaneously silences the expression of all four *Ago* family members in MSCs. **(A)** Schematic depiction of the five-siRNA-containing multiplex retroviral vector pSEB-simAgo2134 and the selected siRNA sequences for individual *Ago* genes. The multiplex siRNA construct was accomplished by using our recently developed FAMSi system **(B)** Multiplex siRNA vector sim*Ago*2134 effectively silences the expression of four *Ago* genes in MSCs. Retroviral stable lines imBMSC-simAgo2134 and imBMSC-siControl cells were first established. Total RNA was isolated from subconfluent imBMSC-siControl and imBMSC-sim*Ago*2134 cells and subjected to TqPCR analysis of the expression of mouse *Ago1*, *Ago2*, *Ago3*, and *Ago4*. Each assay condition was done in triplicate. *Gapdh* was used as a reference gene. **, $P < 0.01$, compared with that of the siControl group.

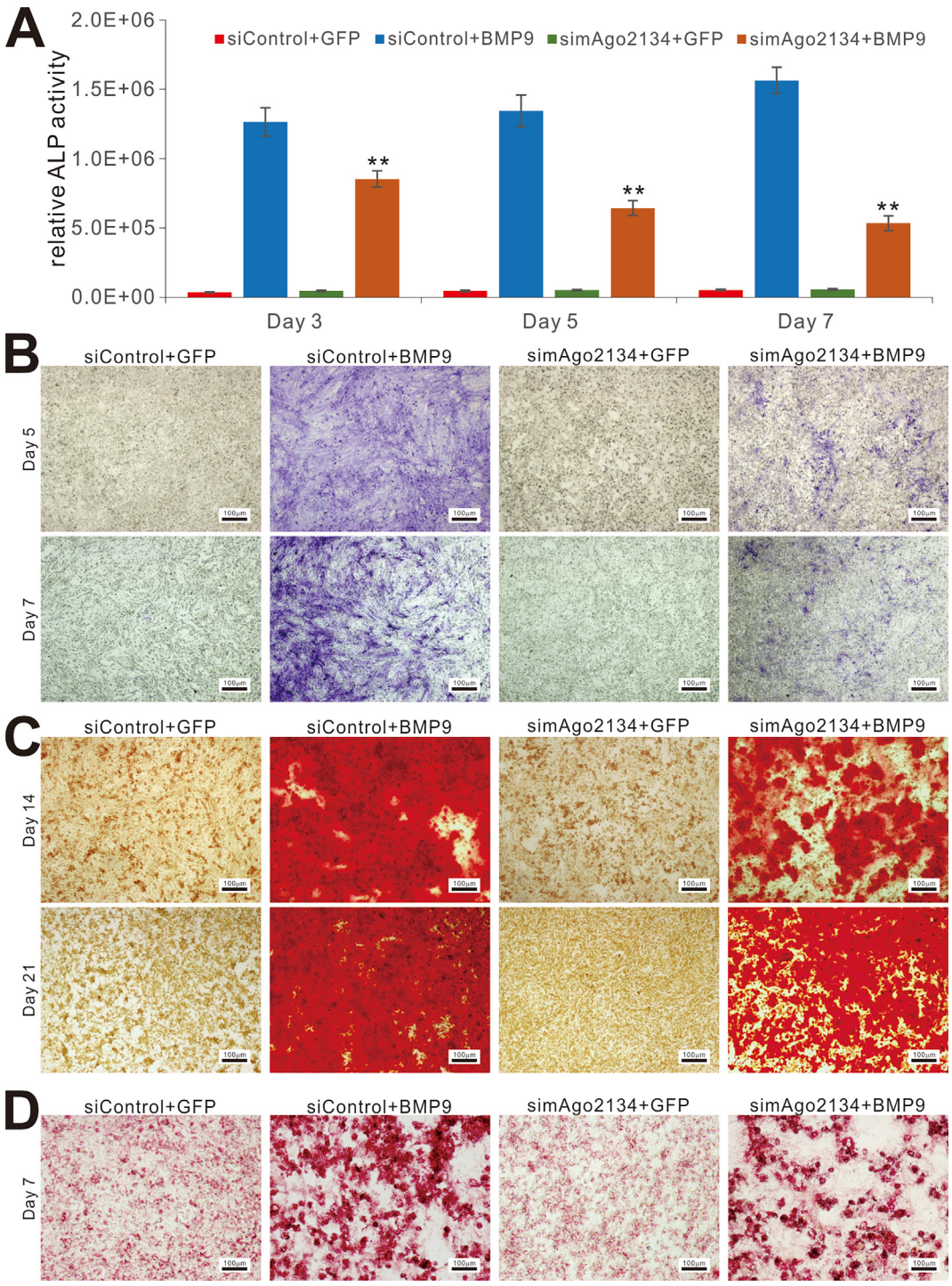

Figure 4 Silencing the expression of the *Ago* family members diminishes BMP9-induced osteogenic and adipogenic differentiation of MSCs. **(A—C)** Silencing the expression of the Ago family members diminishes BMP9-induced ALP activity and matrix mineralization in MSCs. Subconfluent imBMSC-siControl and imBMSC-*Ago*2134 cells were infected with AdGFP or AdBMP9. At 3, 5, and 7 days after infection, ALP activity was determined quantitatively (**A**) and histochemically (**B**). At 14, 21 days after infection, the cells were fixed and subjected to Alizarin Red S staining (**C**). Each assay condition was done in triplicate. Representative images are shown. **, $P < 0.01$, compared with that of the siControl + BMP9 group (**D**) Silencing *Ago* family members reduces BMP9-induced adipogenic differentiation of MSCs. Subconfluent imBMSC-siControl and imBMSC-*Ago*2134 cells were infected with AdGFP or AdBMP9. At 7 days after infection, the cells were fixed and subjected to Oil Red O staining. Representative images are shown. Each assay condition was done in triplicate.

demonstrated that individual sim*Ago* adenoviruses effectively silenced the expression of respective *Ago* genes (Fig. 1D, panels a-d).

Silencing individual *Ago* family members diminishes BMP9-induced early osteogenic marker ALP in MSCs

Using the AdR-sim*Ago* adenoviruses constructed above, we analyzed the effect of individual *Ago* members on BMP9-induced osteogenic differentiation of MSCs. When imBMSC cells were effectively co-infected with AdR-sim*Ago* or AdRFP, and AdBMP9 or AdGFP (Fig. 2A—D, panel a), BMP9-induced ALP activities were significantly decreased in the AdR-sim*Ago* infection groups at the tested time points, compared with that of the AdRFP groups (Fig. 2A—D, panel b). Among the four *Ago* genes, silencing *Ago*2, and to a lesser extent, *Ago*3, led to the most significant reduction of BMP9-induced ALP activity in imBMSC cells, while smaller decreases in ALP activity were observed in *Ago*1 and *Ago*4 knockdown groups (Fig. 2B—b and 2C-b *vs*. 2A-b and 2D-b). Collectively, these findings reveal that *Ago*2 and *Ago*3 play an important role in mediating BMP9-induced osteogenic signaling in MSCs.

Simultaneously silencing the expression of all four *Ago* family members significantly diminishes BMP9-induced osteogenic and adipogenic differentiation in MSCs

To further investigate whether the *Ago* expression was required for BMP9-induced lineage-specific differentiation of MSCs, we sought to construct a retroviral vector expressing five siRNAs, e.g., sim*Ago*2134, two of which target *Ago2* and one each for *Ago1*, *Ago3* and *Ago4*, respectively (Fig. 3A). This retroviral vector was used to establish the stable MSC line imBMSC-sim*Ago*2134, whereas imBMSC-siControl cells were established as a control line. Quantitative qPCR analysis indicates that the expression of all four *Ago* members was effectively silenced in the imBMSC-sim*Ago*2134 cells, compared with that in the control imBMSC-siControl cells (Fig. 3B).

When these stable lines were infected with AdBMP9, both quantitative and qualitative measurements revealed that the ALP activity significantly decreased in the imBMSC-sim*Ago*2134 cells, compared with that of the control imBMSC-siControl cells (Fig. 4A and B). Furthermore, silencing *Ago* expression was shown to significantly decrease BMP9-induced *in vitro* matrix mineralization in the imBMSC-sim*Ago*2134 cells, compared with that of the control imBMSC-siControl cells (Fig. 4C), indicating that AGO proteins are important for both early and late stage of BMP9-induced osteogenic differentiation of MSCs. As BMP9 also induces adipogenic differentiation,[83] we also examined whether BMP9-induced adipogenic differentiation would be impacted when the expression of the *Ago* genes was silenced. As shown in Fig. 4D, silencing *Ago* expression decreased BMP9-induced adipogenic differentiation of MSCs as revealed by Oil Red O staining.

We further analyzed the impact of *Ago* silencing on the expression of the key BMP9-regulated lineage-specific transcriptional factors Runx2 (osteogenic), Sox9 (chondrogenic) and Pparγ (adipogenic) in MSCs.[24,25,83] As expected, while BMP9 simulation significantly up-regulated the expression of Runx2, Sox9 and Pparγ in the imBMSC-siControl cells, compared with that of the GFP groups, silencing *Ago* expression effectively decreased the expression of the *Runx2*, *Sox9* and *Pparγ* in the imBMSC-sim*Ago*2134 cells, compared with that of the imBMSC-siControl cells (Fig. 5A). We further analyzed the effect of *Ago* silencing on the expression of common osteogenic markers and found that the BMP9-induced expression of

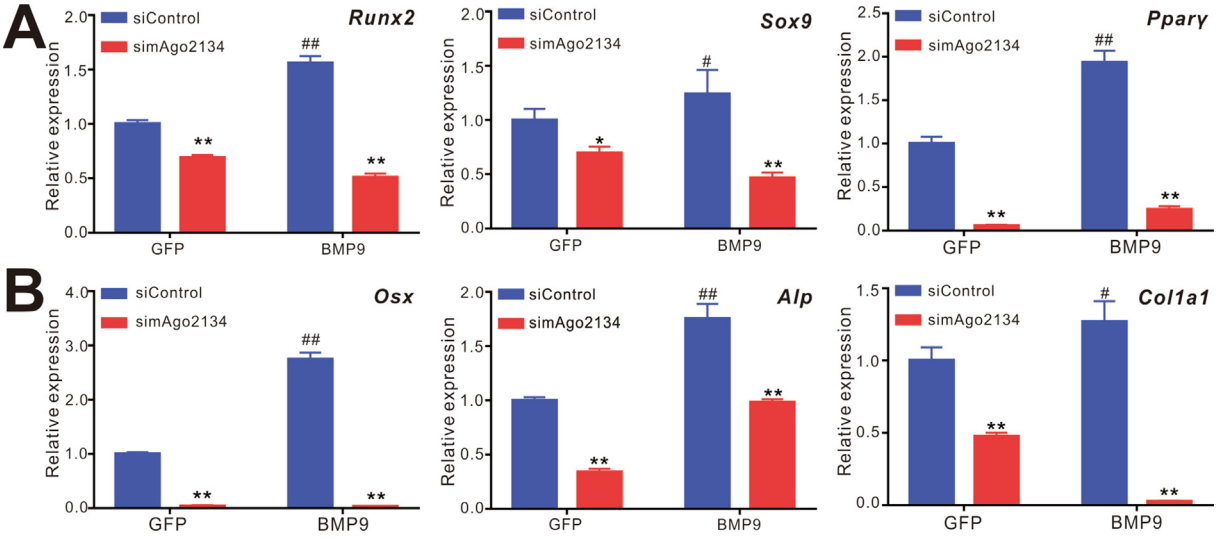

Figure 5 Silencing Ago family members diminishes BMP9-regulated expression of osteogenic and adipogenic differentiation related genes in MSCs. Subconfluent imBMSC-siControl and imBMSC-sim*Ago*2134 cells were infected with AdBMP9 or AdGFP. At 72 h post infection, cells were lysed, and total RNA was isolated and subjected to TqPCR analysis of the expression of MSC lineage-specific regulators including *Runx2, Sox9* and *Pparγ* **(A)** and osteogenic markers including *Osx2, Alp* and *Col1a1* **(B)** *Gapdh* was used as a reference gene. Each assay condition was done in triplicate. *, $P < 0.05$ and **, $P < 0.01$, compared with that of the siControl group. #, $P < 0.05$ and ##, $P < 0.01$, compared with that of the GFP group.

Osx, *Alp* and *Col1a1* was significantly reduced in the imBMSC-sim*Ago*2134 cells, compared with that of the imBMSC-siControl cells (Fig. 5B). Collectively, these results demonstrate that silencing *Ago* significantly diminishes BMP9-induced lineage-specific, especially osteogenic and adipogenic differentiation of MSCs.

Silencing *Ago* family members inhibits BMP9-induced ectopic bone formation *in vivo*

Lastly, we analyzed whether silencing *Ago* expression would impact BMP9-induced bone formation *in vivo*. Using the MSC implantation assay, we found that, upon BMP stimulation, the ectopic bony masses were slightly smaller and much softer in the imBMSC-sim*Ago*2134 injection group, than that of the imBMSC-siControl injection group (Fig. 6A, panel a). MicroCT imaging analysis indicated that silencing *Ago* expression led to a significant decrease in bone mineral density and average bone volume in the imBMSC-sim*Ago*2134 injection group, compared with that of the imBMSC-siControl injection group (Fig. 6A, panel a and b). Histologic evaluation revealed that silencing *Ago* expression significantly decreased mature bone formation in the imBMSC-sim*Ago*2134 injection group, compared with that of the imBMSC-siControl injection group (Fig. 6B, panel a), which was further confirmed by Masson's Trichrome staining (Fig. 6B, panel b). Collectively, these *in vivo* results were supportive of the *in vitro* findings, strongly indicating that *Ago*-mediated microRNA biogenesis plays an essential role in BMP9-induced osteogenic differentiation of MSCs.

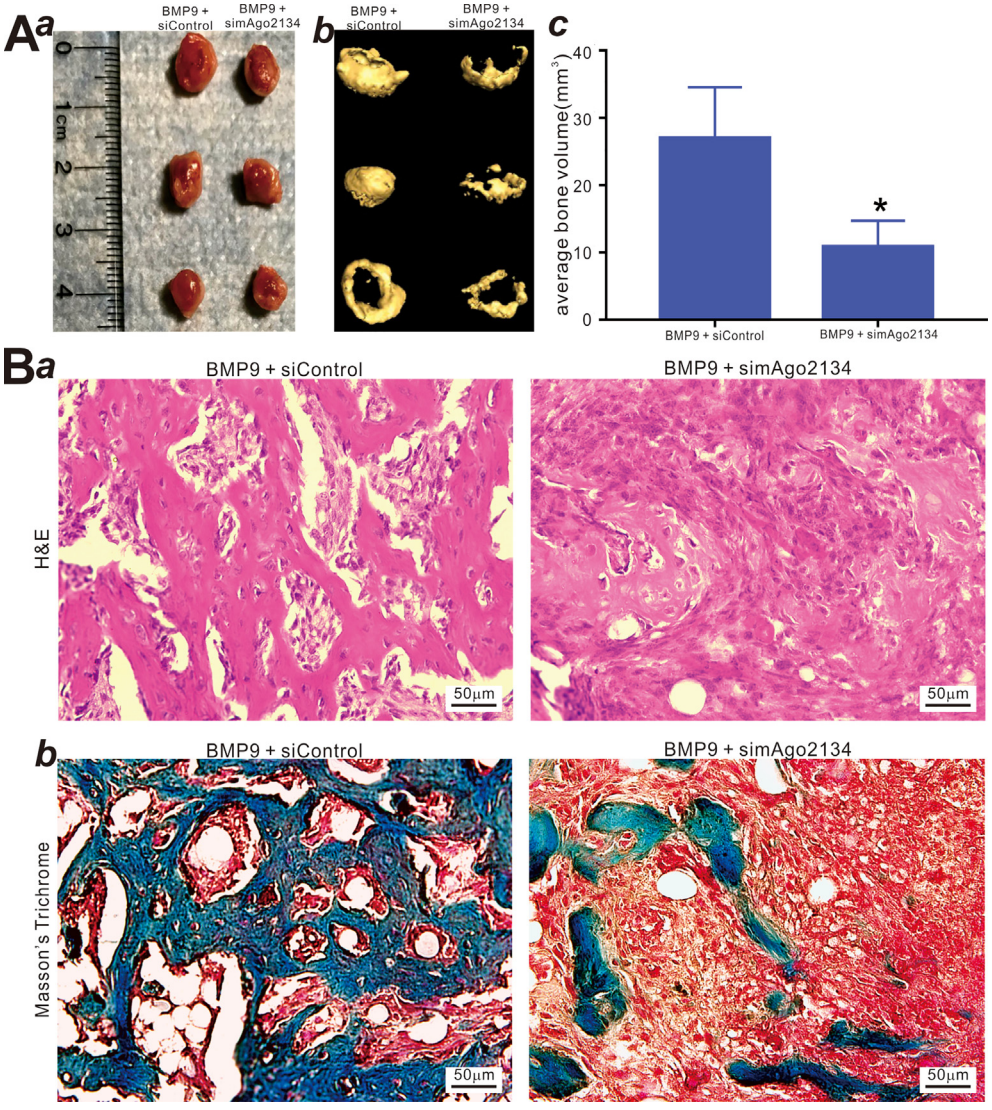

Figure 6 Silencing Ago family members attenuates BMP9-induced ectopic bone formation *in vivo*. **(A)** Subconfluent imBMSC-siControl and imBMSC-sim*Ago*2134 cells were infected with AdBMP9 or AdGFP for 36 h and collected for subcutaneous injection into the flanks of athymic nude mice. At 3 weeks after implantation, the mice were sacrificed and ectopic bone masses were retrieved. No retrievable masses were found in the AdGFP group. Representative gross images **(a)** and micro-CT iso-surface 3D reconstruction **(b)** are shown. The average bone volumes were quantitatively analyzed by using the Amira software **(c)**. *, $P < 0.05$, compared with that of the siControl + BMP9 group. **(B)** H & E and Masson's Trichrome staining. The retrieved masses were fixed, decalcified and subjected to H & E staining **(a)** and Masson's trichrome staining **(b)**. Representative images are shown.

Discussion

We have previously demonstrated that BMP9 is not only the most potent osteogenic factor but also induces adipogenic and chondrogenic differentiation in MSCs.[14,16,18,19,21,83] Our subsequent studies revealed that BMP9 binds to ALK1/2 type I receptors and regulates a panel of downstream target genes, as well as cross-talking with several major signaling pathways in MSCs.[12,15,24–30,64,66,88,97–99] However, the exact mechanism through which BMP9 regulates lineage-specific differentiation of MSCs remains to be elucidated. In this study, through a comprehensive multiplex siRNA-based silencing expression analysis of both individual *Ago* genes, or all four *Ago* genes, we have demonstrated that AGO proteins are important mediators of BMP9-induced osteogenic and adipogenic differentiation in MSCs, indicating that noncoding RNAs, especially microRNAs participate in BMP9-regulated lineage commitment in MSCs.

Noncoding RNAs, particularly miRNAs, have been implicated in bone formation and/or skeletal homeostasis.[38,39,100–105] However, how noncoding RNAs or miRNAs exert their impact on osteogenesis remains to be fully investigated. In this study, we found that BMP9 up-regulated *Ago1*, *Ago2* and *Ago3* in MSCs at the immediate early stage, indicating that regulating *Ago* gene expression provides at least a plausible mechanism to govern miRNA biogenesis and thus regulate miRNA functions in osteogenic differentiation. Alternatively, BMP9 may regulate miRNAs that target other lncRNAs and/or signaling pathways, thus indirectly mediating BMP9 osteogenic signaling. In fact, we have recently found that upon BMP9 stimulation lncRNA H19 was upregulated in MSCs at the early stage and then decreased rapidly, followed by a gradual return to basal expression. Notably, H19 overexpression or H19 expression knockdown in MSCs interrupted BMP9-induced osteogenesis, which can be rescued by activated Notch signaling.[65] We further revealed that H19 might modulate Notch pathway-targeting miRNAs and then indirectly impact BMP9 signaling in MSCs.[64,65] It has been reported that several miRNAs, including miR-133, miR-135, miR-206, miR-141 and miR-200a, miR-208, miR-125b, miR-204, miR-26a, miR-29, miR-27 and miR-2861, regulate the BMP-mediated induction of osteoblastic differentiation.[102] Furthermore, miRNAs may regulate osteoblast and osteoclast lineage-specific transcription factors, and orchestrate feedforward and reverse loops of signaling pathways and regulatory networks, leading to control of normal bone formation and turnover. Thus, miRNA deregulation may impact the progression of bone-related disorders including osteoporosis.[38,39]

AGOs are conserved and specialized smRNA-binding proteins for miRNAs, siRNAs or PIWI-associated RNAs (i.e., piRNAs), leading to silencing target mRNAs by interacting with other factors.[46,106,107] Thus, AGO proteins serve as a major component of the RISCs with small RNAs and other proteins such as Dicer, GW182 proteins, and Hsp70/Hsp90.[106] Four AGO proteins (AGO1–4) in humans and mice are conserved at the amino acid level with 99% for AGO2, 3, and 4 and 100% for AGO1 between mouse and human.[107] The *Ago2* knockout mice were lethal during early development at post-implantation stages, whereas *Ago1, 3,* and *4* knockout mice are viable.[107] Nonetheless, the phenotype of the *Ago2*-deficient mice compared to other RNAi-deficient mice, e.g., *Dicer*- or *Drosha*-deficient mice, is not identical, indicating distinct regulatory roles for the RNAi or RISC effectors during mouse development.[107] In fact, emerging evidence indicates that the biological functions of AGO-associated smRNAs expand beyond the post-transcriptional regulation by miRNAs, and are implicated in transcriptional gene silencing or activation, alternative splicing, antiviral defense, genome integrity control, DNA repair, and epigenetic modifications.[107] An early *in vitro* study showed that silencing *DICER* or *DROSHA* in human MSCs inhibited osteogenic differentiation.[108] Thus, it is conceivable AGO proteins and the associated smRNAs, especially miRNAs, may play an essential role in modulating lineage commitments and tissue-specific terminal differentiation of MSCs, and bone homeostasis, although many detailed mechanisms have yet to be uncovered.

In summary, we examined the potential roles of AGO proteins in BMP9-induced lineage-specific differentiation of MSCs. Using multiplex siRNA vectors to express multiple siRNAs silencing individual *Ago* genes or all four *Ago* genes, we demonstrated that the expression of *Ago1*, *Ago2* and *Ago3* was up-regulated by BMP9 in MSCs and that silencing individual *Ago* expression decreased BMP9-induced ALP activity in MSCs. We further demonstrated that simultaneous silencing of all four Ago genes effectively diminished osteogenic and adipogenic differentiation in MSCs, *in vitro* matrix mineralization, and *in vivo* ectopic bone formation induced by BMP9. Taken together, our results strongly suggest that AGO proteins and associated small RNA biogenesis pathway may be essential for BMP9-induced osteogenic differentiation of MSCs.

Authors contribution

HHL, TCH, LC, JY, LS and YM conceived and designed the study. YM, NN, LH, JF, HW and FH performed the experiments and collected data. QL, DS, KF, MP, WW, ABT and CC participated in molecular cloning experiments; provided essential experimental materials; and assisted in histological preparations and staining, and qPCR data analysis and interpretations. YM, LC, RRR, HHL, RCH, SHH, MJL, JY, LS and TCH drafted and revised the manuscript. All authors read, reviewed and approved the final manuscript.

Conflict of Interests

The authors declare no competing conflicts of interest.

Funding

The authors wish to thank Dr. Aaron Hsiu-Ming Tsai of the Integrated Small Animal Imaging Research Resource (iSAIRR) Faculty at The University of Chicago, for his valuable and resourceful support. The reported work was supported in part by research grants from the National Institutes of Health (CA226303 to TCH, and AR072731 to JY), the Chicago Biomedical Consortium with support from the Searle Funds at The Chicago Community Trust (RRR),

and the Scoliosis Research Society (TCH and MJL). WW was supported by the Medical Scientist Training Program of the National Institutes of Health (T32 GM007281). This project was also supported in part by The University of Chicago Cancer Center Support Grant (P30CA014599) and the National Center for Advancing Translational Sciences (NCATS) of the National Institutes of Health (NIH) through Grant Number 5UL1TR002389-02 that funds the Institute for Translational Medicine (ITM). TCH was supported by the Mabel Green Myers Research Endowment Fund and The University of Chicago Orthopaedics Alumni Fund. Funding sources were not involved in the study design; in the collection, analysis and/or interpretation of data; in the writing of the report; or in the decision to submit the paper for publication.

Appendix A. Supplementary data

Supplementary data to this article can be found online at https://doi.org/10.1016/j.gendis.2021.04.004.

References

1. Prockop DJ. Marrow stromal cells as stem cells for nonhematopoietic tissues. *Science*. 1997;276(5309):71—74.
2. Deng ZL, Sharff KA, Tang N, et al. Regulation of osteogenic differentiation during skeletal development. *Front Biosci*. 2008;13:2001—2021.
3. Rastegar F, Shenaq D, Huang J, et al. Mesenchymal stem cells: molecular characteristics and clinical applications. *World J Stem Cells*. 2010;2(4):67—80.
4. Shenaq DS, Rastegar F, Petkovic D, et al. Mesenchymal progenitor cells and their orthopedic applications: forging a path towards clinical trials. *Stem Cell Int*. 2010;2010, e519028.
5. Teven CM, Liu X, Hu N, et al. Epigenetic regulation of mesenchymal stem cells: a focus on osteogenic and adipogenic differentiation. *Stem Cells Int*. 2011;2011, e201371.
6. Raucci A, Bellosta P, Grassi R, Basilico C, Mansukhani A. Osteoblast proliferation or differentiation is regulated by relative strengths of opposing signaling pathways. *J Cell Physiol*. 2008;215(2):442—451.
7. Kim JH, Liu X, Wang J, et al. Wnt signaling in bone formation and its therapeutic potential for bone diseases. *Ther Adv Musculoskelet Dis*. 2013;5(1):13—31.
8. Yang K, Wang X, Zhang H, et al. The evolving roles of canonical WNT signaling in stem cells and tumorigenesis: implications in targeted cancer therapies. *Lab Invest*. 2016;96(2):116—136.
9. Denduluri SK, Idowu O, Wang Z, et al. Insulin-like growth factor (IGF) signaling in tumorigenesis and the development of cancer drug resistance. *Genes Dis*. 2015;2(1):13—25.
10. Teven CM, Farina EM, Rivas J, Reid RR. Fibroblast growth factor (FGF) signaling in development and skeletal diseases. *Genes Dis*. 2014;1(2):199—213.
11. Jo A, Denduluri S, Zhang B, et al. The versatile functions of Sox9 in development, stem cells, and human diseases. *Genes Dis*. 2014;1(2):149—161.
12. Zhang F, Song J, Zhang H, et al. Wnt and BMP signaling crosstalk in regulating dental stem cells: implications in dental tissue engineering. *Genes Dis*. 2016;3(4):263—276.
13. Zhang L, Luo Q, Shu Y, et al. Transcriptomic landscape regulated by the 14 types of bone morphogenetic proteins (BMPs) in lineage commitment and differentiation of mesenchymal stem cells (MSCs). *Genes Dis*. 2019;6(3):258—275.
14. Luu HH, Song WX, Luo X, et al. Distinct roles of bone morphogenetic proteins in osteogenic differentiation of mesenchymal stem cells. *J Orthop Res*. 2007;25(5):665—677.
15. Wang RN, Green J, Wang Z, et al. Bone Morphogenetic Protein (BMP) signaling in development and human diseases. *Genes Dis*. 2014;1(1):87—105.
16. Mostafa S, Pakvasa M, Coalson E, et al. The wonders of BMP9: from mesenchymal stem cell differentiation, angiogenesis, neurogenesis, tumorigenesis, and metabolism to regenerative medicine. *Genes Dis*. 2019;6(3):201—223.
17. Liu W, Deng Z, Zeng Z, et al. Highly expressed BMP9/GDF2 in postnatal mouse liver and lungs may account for its pleiotropic effects on stem cell differentiation, angiogenesis, tumor growth and metabolism. *Genes Dis*. 2019;7(2):235—244.
18. Cheng H, Jiang W, Phillips FM, et al. Osteogenic activity of the fourteen types of human bone morphogenetic proteins (BMPs). *J Bone Joint Surg Am*. 2003;85(8):1544—1552.
19. Kang Q, Sun MH, Cheng H, et al. Characterization of the distinct orthotopic bone-forming activity of 14 BMPs using recombinant adenovirus-mediated gene delivery. *Gene Ther*. 2004;11(17):1312—1320.
20. Luther G, Wagner ER, Zhu G, et al. BMP-9 induced osteogenic differentiation of mesenchymal stem cells: molecular mechanism and therapeutic potential. *Curr Gene Ther*. 2011;11(3):229—240.
21. Lamplot JD, Qin J, Nan G, et al. BMP9 signaling in stem cell differentiation and osteogenesis. *Am J Stem Cells*. 2013;2(1):1—21.
22. Wang Y, Hong S, Li M, et al. Noggin resistance contributes to the potent osteogenic capability of BMP9 in mesenchymal stem cells. *J Orthop Res*. 2013;31(11):1796—1803.
23. Luo J, Tang M, Huang J, et al. TGFbeta/BMP type I receptors ALK1 and ALK2 are essential for BMP9-induced osteogenic signaling in mesenchymal stem cells. *J Biol Chem*. 2010;285(38):29588—29598.
24. Peng Y, Kang Q, Cheng H, et al. Transcriptional characterization of bone morphogenetic proteins (BMPs)-mediated osteogenic signaling. *J Cell Biochem*. 2003;90(6):1149—1165.
25. Peng Y, Kang Q, Luo Q, et al. Inhibitor of DNA binding/differentiation helix-loop-helix proteins mediate bone morphogenetic protein-induced osteoblast differentiation of mesenchymal stem cells. *J Biol Chem*. 2004;279(31):32941—32949.
26. Luo Q, Kang Q, Si W, et al. Connective tissue growth factor (CTGF) is regulated by Wnt and bone morphogenetic proteins signaling in osteoblast differentiation of mesenchymal stem cells. *J Biol Chem*. 2004;279(53):55958—55968.
27. Sharff KA, Song WX, Luo X, et al. Hey1 basic helix-loop-helix protein plays an important role in mediating BMP9-induced osteogenic differentiation of mesenchymal progenitor cells. *J Biol Chem*. 2009;284(1):649—659.
28. Huang E, Zhu G, Jiang W, et al. Growth hormone synergizes with BMP9 in osteogenic differentiation by activating the JAK/STAT/IGF1 pathway in murine multilineage cells. *J Bone Miner Res*. 2012;27(7):1566—1575.
29. Wang J, Liao J, Zhang F, et al. NEL-like molecule-1 (Nell1) is regulated by bone morphogenetic protein 9 (BMP9) and potentiates BMP9-induced osteogenic differentiation at the expense of adipogenesis in mesenchymal stem cells. *Cell Physiol Biochem*. 2017;41(2):484—500.
30. Wang J, Zhang H, Zhang W, et al. Bone morphogenetic protein-9 effectively induces osteo/odontoblastic differentiation of the reversibly immortalized stem cells of dental apical papilla. *Stem Cells Dev*. 2014;23(12):1405—1416.
31. Si W, Kang Q, Luu HH, et al. CCN1/Cyr61 is regulated by the canonical Wnt signal and plays an important role in Wnt3A-

induced osteoblast differentiation of mesenchymal stem cells. *Mol Cell Biol*. 2006;26(8):2955—2964.
32. Brosnan CA, Voinnet O. The long and the short of noncoding RNAs. *Curr Opin Cell Biol*. 2009;21(3):416—425.
33. Cech TR, Steitz JA. The noncoding RNA revolution-trashing old rules to forge new ones. *Cell*. 2014;157(1):77—94.
34. Quinn JJ, Chang HY. Unique features of long non-coding RNA biogenesis and function. *Nat Rev Genet*. 2016;17(1):47—62.
35. Mattick JS, Makunin IV. Non-coding RNA. *Hum Mol Genet*. 2006;15(Spec No 1):R17—R29.
36. Lee RC, Feinbaum RL, Ambros V. The C. elegans heterochronic gene lin-4 encodes small RNAs with antisense complementarity to lin-14. *Cell*. 1993;75(5):843—854.
37. Wightman B, Ha I, Ruvkun G. Posttranscriptional regulation of the heterochronic gene lin-14 by lin-4 mediates temporal pattern formation in C. elegans. *Cell*. 1993;75(5):855—862.
38. Lian JB, Stein GS, van Wijnen AJ, et al. MicroRNA control of bone formation and homeostasis. *Nat Rev Endocrinol*. 2012;8(4):212—227.
39. Bellavia D, De Luca A, Carina V, et al. Deregulated miRNAs in bone health: epigenetic roles in osteoporosis. *Bone*. 2019;122:52—75.
40. Soifer HS, Rossi JJ, Saetrom P. MicroRNAs in disease and potential therapeutic applications. *Mol Ther*. 2007;15(12):2070—2079.
41. Gebert LFR, MacRae IJ. Regulation of microRNA function in animals. *Nat Rev Mol Cell Biol*. 2019;20(1):21—37.
42. Treiber T, Treiber N, Meister G. Regulation of microRNA biogenesis and its crosstalk with other cellular pathways. *Nat Rev Mol Cell Biol*. 2019;20(1):5—20.
43. Zamore PD, Tuschl T, Sharp PA, Bartel DP. RNAi: double-stranded RNA directs the ATP-dependent cleavage of mRNA at 21 to 23 nucleotide intervals. *Cell*. 2000;101(1):25—33.
44. Tomari Y, Zamore PD. Perspective: machines for RNAi. *Genes Dev*. 2005;19(5):517—529.
45. Bobbin ML, Rossi JJ. RNA interference (RNAi)-Based therapeutics: delivering on the promise? *Annu Rev Pharmacol Toxicol*. 2016;56:103—122.
46. Meister G. Argonaute proteins: functional insights and emerging roles. *Nat Rev Genet*. 2013;14(7):447—459.
47. He F, Ni N, Zeng Z, et al. FAMSi: a synthetic biology approach to the fast assembly of multiplex siRNAs for silencing gene expression in mammalian cells. *Mol Ther Nucleic Acids*. 2020;22:885—899.
48. Wu N, Zhang H, Deng F, et al. Overexpression of Ad5 precursor terminal protein accelerates recombinant adenovirus packaging and amplification in HEK-293 packaging cells. *Gene Ther*. 2014;21(7):629—637.
49. Wei Q, Fan J, Liao J, et al. Engineering the rapid adenovirus production and amplification (RAPA) cell line to expedite the generation of recombinant adenoviruses. *Cell Physiol Biochem*. 2017;41(6):2383—2398.
50. Hu X, Li L, Yu X, et al. CRISPR/Cas9-mediated reversibly immortalized mouse bone marrow stromal stem cells (BMSCs) retain multipotent features of mesenchymal stem cells (MSCs). *Oncotarget*. 2017;8(67):111847—111865.
51. Yu X, Chen L, Wu K, et al. Establishment and functional characterization of the reversibly immortalized mouse glomerular podocytes (imPODs). *Genes Dis*. 2018;5(2):137—149.
52. Yan S, Zhang R, Wu K, et al. Characterization of the essential role of bone morphogenetic protein 9 (BMP9) in osteogenic differentiation of mesenchymal stem cells (MSCs) through RNA interference. *Genes Dis*. 2018;5(2):172—184.
53. Zeng Z, Huang B, Huang S, et al. The development of a sensitive fluorescent protein-based transcript reporter for high throughput screening of negative modulators of lncRNAs. *Genes Dis*. 2018;5(1):62—74.
54. Zeng Z, Huang B, Wang X, et al. A reverse transcriptase-mediated ribosomal RNA depletion (RTR2D) strategy for the cost-effective construction of RNA sequencing libraries. *J Adv Res*. 2020;24:239—250.
55. Luo J, Deng ZL, Luo X, et al. A protocol for rapid generation of recombinant adenoviruses using the AdEasy system. *Nat Protoc*. 2007;2(5):1236—1247.
56. Lee CS, Bishop ES, Zhang R, et al. Adenovirus-mediated gene delivery: potential applications for gene and cell-based therapies in the new era of personalized medicine. *Genes Dis*. 2017;4(2):43—63.
57. Huang E, Bi Y, Jiang W, et al. Conditionally immortalized mouse embryonic fibroblasts retain proliferative activity without compromising multipotent differentiation potential. *PLoS One*. 2012;7(2), e32428.
58. Wang X, Yuan C, Huang B, et al. Developing a versatile shotgun cloning strategy for single-vector-based multiplex expression of short interfering RNAs (siRNAs) in mammalian cells. *ACS Synth Biol*. 2019;8(9):2092—2105.
59. Zhang B, Yang L, Zeng Z, et al. Leptin potentiates BMP9-induced osteogenic differentiation of mesenchymal stem cells through the activation of JAK/STAT signaling. *Stem Cells Dev*. 2020;29(8):498—510.
60. Luo Q, Kang Q, Song WX, et al. Selection and validation of optimal siRNA target sites for RNAi-mediated gene silencing. *Gene*. 2007;395(1—2):160—169.
61. Deng F, Chen X, Liao Z, et al. A simplified and versatile system for the simultaneous expression of multiple siRNAs in mammalian cells using Gibson DNA Assembly. *PLoS One*. 2014;9(11), e113064.
62. Fan J, Feng Y, Zhang R, et al. A simplified system for the effective expression and delivery of functional mature microRNAs in mammalian cells. *Cancer Gene Ther*. 2020;27(6):424—437.
63. Fan J, Wei Q, Liao J, et al. Noncanonical Wnt signaling plays an important role in modulating canonical Wnt-regulated stemness, proliferation and terminal differentiation of hepatic progenitors. *Oncotarget*. 2017;8(16):27105—27119.
64. Liao J, Wei Q, Zou Y, et al. Notch signaling augments BMP9-induced bone formation by promoting the osteogenesis-angiogenesis coupling process in mesenchymal stem cells (MSCs). *Cell Physiol Biochem*. 2017;41(5):1905—1923.
65. Liao J, Yu X, Hu X, et al. lncRNA H19 mediates BMP9-induced osteogenic differentiation of mesenchymal stem cells (MSCs) through Notch signaling. *Oncotarget*. 2017;8(32):53581—53601.
66. Zhang H, Wang J, Deng F, et al. Canonical Wnt signaling acts synergistically on BMP9-induced osteo/odontoblastic differentiation of stem cells of dental apical papilla (SCAPs). *Biomaterials*. 2015;39:145—154.
67. Zhang J, Weng Y, Liu X, et al. Endoplasmic reticulum (ER) stress inducible factor cysteine-rich with EGF-like domains 2 (Creld2) is an important mediator of BMP9-regulated osteogenic differentiation of mesenchymal stem cells. *PLoS One*. 2013;8(9), e73086.
68. Li Y, Wagner ER, Yan Z, et al. The calcium-binding protein S100A6 accelerates human osteosarcoma growth by promoting cell proliferation and inhibiting osteogenic differentiation. *Cell Physiol Biochem*. 2015;37(6):2375—2392.
69. Shu Y, Yang C, Ji X, et al. Reversibly immortalized human umbilical cord-derived mesenchymal stem cells (UC-MSCs) are responsive to BMP9-induced osteogenic and adipogenic differentiation. *J Cell Biochem*. 2018;119(11):8872—8886.

70. Zhao C, Wu N, Deng F, et al. Adenovirus-mediated gene transfer in mesenchymal stem cells can be significantly enhanced by the cationic polymer polybrene. *PLoS One*. 2014;9(3), e92908.
71. Shu Y, Wu K, Zeng Z, et al. A simplified system to express circularized inhibitors of miRNA for stable and potent suppression of miRNA functions. *Mol Ther Nucleic Acids*. 2018;13:556—567.
72. Liao J, Wei Q, Fan J, et al. Characterization of retroviral infectivity and superinfection resistance during retrovirus-mediated transduction of mammalian cells. *Gene Ther*. 2017;24(6):333—341.
73. Bi Y, He Y, Huang J, et al. Functional characteristics of reversibly immortalized hepatic progenitor cells derived from mouse embryonic liver. *Cell Physiol Biochem*. 2014;34(4):1318—1338.
74. Bi Y, Huang J, He Y, et al. Wnt antagonist SFRP3 inhibits the differentiation of mouse hepatic progenitor cells. *J Cell Biochem*. 2009;108(1):295—303.
75. Huang J, Bi Y, Zhu GH, et al. Retinoic acid signalling induces the differentiation of mouse fetal liver-derived hepatic progenitor cells. *Liver Int*. 2009;29(10):1569—1581.
76. Untergasser A, Cutcutache I, Koressaar T, et al. Primer3-new capabilities and interfaces. *Nucleic Acids Res*. 2012;40(15),e115.
77. Zhang Q, Wang J, Deng F, et al. TqPCR: a touchdown qPCR assay with significantly improved detection sensitivity and amplification efficiency of SYBR green qPCR. *PLoS One*. 2015; 10(7), e0132666.
78. Liu X, Qin J, Luo Q, et al. Cross-talk between EGF and BMP9 signalling pathways regulates the osteogenic differentiation of mesenchymal stem cells. *J Cell Mol Med*. 2013;17(9):1160—1172.
79. Wang N, Zhang W, Cui J, et al. The piggyBac transposon-mediated expression of SV40 T antigen efficiently immortalizes mouse embryonic fibroblasts (MEFs). *PLoS One*. 2014;9(5), e97316.
80. Zhang Z, Liu J, Zeng Z, et al. lncRNA Rmst acts as an important mediator of BMP9-induced osteogenic differentiation of mesenchymal stem cells (MSCs) by antagonizing Notch-targeting microRNAs. *Aging (Albany NY)*. 2019;11(24): 12476—12496.
81. Zhao C, Qazvini NT, Sadati M, et al. A pH-triggered, self-assembled, and bioprintable hybrid hydrogel scaffold for mesenchymal stem cell based bone tissue engineering. *ACS Appl Mater Interfaces*. 2019;11(9):8749—8762.
82. Zhao C, Zeng Z, Qazvini NT, et al. Thermoresponsive citrate-based graphene oxide scaffold enhances bone regeneration from BMP9-stimulated adipose-derived mesenchymal stem cells. *ACS Biomater Sci Eng*. 2018;4(8):2943—2955.
83. Kang Q, Song WX, Luo Q, et al. A comprehensive analysis of the dual roles of BMPs in regulating adipogenic and osteogenic differentiation of mesenchymal progenitor cells. *Stem Cell Dev*. 2009;18(4):545—559.
84. Wang H, Cao Y, Shu L, et al. Long non-coding RNA (lncRNA) H19 induces hepatic steatosis through activating MLXIPL and mTORC1 networks in hepatocytes. *J Cell Mol Med*. 2020;24(2):1399—1412.
85. Song D, Zhang F, Reid RR, et al. BMP9 induces osteogenesis and adipogenesis in the immortalized human cranial suture progenitors from the patent sutures of craniosynostosis patients. *J Cell Mol Med*. 2017;21(11):2782—2795.
86. Cui J, Zhang W, Huang E, et al. BMP9-induced osteoblastic differentiation requires functional Notch signaling in mesenchymal stem cells. *Lab Invest*. 2019;99(1):58—71.
87. Gao Y, Huang E, Zhang H, et al. Crosstalk between Wnt/beta-catenin and estrogen receptor signaling synergistically promotes osteogenic differentiation of mesenchymal progenitor cells. *PLoS One*. 2013;8(12), e82436.
88. Zhang W, Deng ZL, Chen L, et al. Retinoic acids potentiate BMP9-induced osteogenic differentiation of mesenchymal progenitor cells. *PLoS One*. 2010;5(7), e11917.
89. Luo X, Chen J, Song WX, et al. Osteogenic BMPs promote tumor growth of human osteosarcomas that harbor differentiation defects. *Lab Invest*. 2008;88(12):1264—1277.
90. Chen L, Jiang W, Huang J, et al. Insulin-like growth factor 2 (IGF-2) potentiates BMP-9-induced osteogenic differentiation and bone formation. *J Bone Miner Res*. 2010;25(11): 2447—2459.
91. Li R, Zhang W, Cui J, et al. Targeting BMP9-promoted human osteosarcoma growth by inactivation of notch signaling. *Curr Cancer Drug Targets*. 2014;14(3):274—285.
92. Ye J, Wang J, Zhu Y, et al. A thermoresponsive polydiolcitrate-gelatin scaffold and delivery system mediates effective bone formation from BMP9-transduced mesenchymal stem cells. *Biomed Mater*. 2016;11(2), e025021.
93. Lamplot JD, Liu B, Yin L, et al. Reversibly immortalized mouse articular chondrocytes acquire long-term proliferative capability while retaining chondrogenic phenotype. *Cell Transplant*. 2015;24(6):1053—1066.
94. Lu S, Wang J, Ye J, et al. Bone morphogenetic protein 9 (BMP9) induces effective bone formation from reversibly immortalized multipotent adipose-derived (iMAD) mesenchymal stem cells. *Am J Transl Res*. 2016;8(9):3710—3730.
95. Shui W, Zhang W, Yin L, et al. Characterization of scaffold carriers for BMP9-transduced osteoblastic progenitor cells in bone regeneration. *J Biomed Mater Res A*. 2014;102(10): 3429—3438.
96. Dumanian ZP, Tollemar V, Ye J, et al. Repair of critical sized cranial defects with BMP9-transduced calvarial cells delivered in a thermoresponsive scaffold. *PLoS One*. 2017;12(3), e0172327.
97. Hu N, Jiang D, Huang E, et al. BMP9-regulated angiogenic signaling plays an important role in the osteogenic differentiation of mesenchymal progenitor cells. *J Cell Sci*. 2013; 126(Pt 2):532—541.
98. Hu N, Wang C, Liang X, et al. Inhibition of histone deacetylases potentiates BMP9-induced osteogenic signaling in mouse mesenchymal stem cells. *Cell Physiol Biochem*. 2013;32(2): 486—498.
99. Pakvasa M, Haravu P, Boachie-Mensah M, et al. Notch signaling: its essential roles in bone and craniofacial development. *Genes Dis*. 2021;8(1):8—24.
100. Papaioannou G, Mirzamohammadi F, Kobayashi T. MicroRNAs involved in bone formation. *Cell Mol Life Sci*. 2014;71(24): 4747—4761.
101. Papaioannou G. miRNAs in bone development. *Curr Genomics*. 2015;16(6):427—434.
102. Kapinas K, Delany AM. MicroRNA biogenesis and regulation of bone remodeling. *Arthritis Res Ther*. 2011;13(3), e220.
103. Ell B, Kang Y. MicroRNAs as regulators of bone homeostasis and bone metastasis. *BoneKEy Rep*. 2014;3,e549.
104. Pi C, Li YP, Zhou X, Gao B. The expression and function of microRNAs in bone homeostasis. *Front Biosci (Landmark Ed)*. 2015;20:119—138.
105. van der Eerden BC. MicroRNAs in the skeleton: cell-restricted or potent intercellular communicators? *Arch Biochem Biophys*. 2014;561:46—55.
106. Wu J, Yang J, Cho WC, Zheng Y. Argonaute proteins: structural features, functions and emerging roles. *J Adv Res*. 2020; 24:317—324.
107. Müller M, Fazi F, Ciaudo C. Argonaute proteins: from structure to function in development and pathological cell fate determination. *Front Cell Dev Biol*. 2020;7,e360.
108. Oskowitz AZ, Lu J, Penfornis P, et al. Human multipotent stromal cells from bone marrow and microRNA: regulation of differentiation and leukemia inhibitory factor expression. *Proc Natl Acad Sci U S A*. 2008;105(47):18372—18377.